

**Calculations of Li adsorption and diffusion on MgO(100) in comparison to Ca**

Lijun Xu and Graeme Henkelman\*

*Department of Chemistry and Biochemistry, University of Texas at Austin, Austin, Texas 78712-0165, USA*

(Received 23 May 2010; published 7 September 2010)

Density-functional theory calculations are used to study the adsorption and growth of small Li clusters on MgO(100). The binding of Li is found to be similar to that of Ca in many respects. Monomers bind to oxygen sites on the terrace and diffuse at room temperature to defect sites. A range of defect sites will bind monomers with increasing energies from oxygen vacancies, steps, kinks, divacancies, and magnesium vacancies, as well as to peroxo species on step edges. The binding strength correlates with the amount of Bader charge transferred from the adsorbing metal to the substrate. Small clusters are found to be highly mobile on the surface at room temperature. In two cases, we have found qualitative differences in the binding energies of Ca and Li which lead to different growth modes. First, Ca binds less strongly to charged oxygen vacancy defects ( $F^+$  centers) than it does on the terrace whereas Li forms a bond with the electron in the vacancy, and is trapped at room temperature. Second, the gas phase Ca dimer distance is longer than the O-O distance on the MgO surface so that epitaxial Ca islands are strained whereas Li is not. These two differences have a profound effect on the growth of clusters. At room temperature, a Ca monomer will not trap at defect sites occupied by another Ca monomer. Thus, Ca atoms diffuse on the terrace until the defects are saturated before nucleating three-dimensional islands. On the other hand, two-dimensional epitaxial Li island nucleate at Li-bound defects. These calculations explain the lower initial heat of adsorption of Li and higher surface coverage as compared to Ca in adsorption microcalorimetry measurements by Farmer *et al.* [*J. Am. Chem. Soc.* **131**, 3098 (2009)].

DOI: [10.1103/PhysRevB.82.115407](https://doi.org/10.1103/PhysRevB.82.115407)

PACS number(s): 68.43.Bc, 68.43.Jk, 68.43.Fg, 68.35.Fx

**I. INTRODUCTION**

Magnesium oxide catalyzes a variety of interesting reactions such as activation of small alkanes<sup>1-4</sup> and is even a possible replacement of the current homogeneous catalyst systems in upgrading triglycerides into biodiesel.<sup>5</sup> In fundamental research, MgO(100) has been widely used to support metal/oxide model catalysts, which also have promising industrial applications.<sup>6-8</sup> Additionally, studies of metal growth on MgO(100) promote the understanding of interactions between metals and surface sites, which is one of the key steps toward tuning the functionality of metal/oxide catalytic systems.

In studies of transition metals on MgO(100), defects are found to be anchoring sites which control nucleation and growth of particles and thin films<sup>6,7,9-14</sup> but there is still debate about which defects are important for different metal/oxide combinations.<sup>15,16</sup> On MgO(100), even the identities and structures of surface defects are in question,<sup>17-22</sup> let alone their role in interface formation. Alkali and alkaline-earth metals have a lower electronegativity than transition metals and bind to MgO in a different way.<sup>23-33</sup> In a recent study of Ca growth on MgO(100),<sup>30</sup> it was shown that this difference can provide information about binding sites which could be overlooked by studies with transition metals. In this work, we investigate Li as the adsorbate to study the role of surface sites in controlling the growth of metal particles and thin films on MgO(100).

Li has been extensively studied as an additive to promote the catalytic activity of MgO(100) for many reactions such as the conversion of methane into ethane or ethylene or other products,<sup>1,34,35</sup> dehydrogenation of propane,<sup>36</sup> and citral condensation with acetone.<sup>37</sup> As well as studies of catalytic activity,<sup>38-43</sup> fundamental studies have been focused on ef-

fects of Li dopants on the electronic, optical, and magnetic properties of MgO.<sup>44-50</sup> In the recent density-functional theory (DFT) study by Scanlon *et al.*,<sup>50</sup> doping of Li in the top layer of MgO(100) was shown to create an unoccupied state with  $O_{2p}$  valence character which assists catalytic hydrogen abstraction. Adsorption of Li atoms on the surface of MgO(100) can also be used to tune the surface geometry and electronic structure. Martinez *et al.*<sup>29</sup> calculated the change in work function upon adsorption of alkali metals with DFT and proposed that a net transfer of the  $2s$  valence electron of Li to the MgO thin films decreases the work function. This is consistent with the formation of paramagnetic surface centers from alkali metals on MgO proposed by Brazzelli *et al.*<sup>23</sup> Lian *et al.* and Finazzi *et al.*<sup>27,28</sup> studied the adsorption of Li atoms and clusters on MgO(100) surface with electron paramagnetic resonance (EPR) spectroscopy (at 35 K) and DFT. They concluded that Li adatoms adsorb mainly at terrace sites with a low density of small clusters formed at lower coordinated sites (such as edges and reverse corners) by fast diffusion of Li adatoms (barrier  $<0.2$  eV). Their calculations showed that a polarization of the charge density from Li to the surface is consistent with the observed  $g$  values and hyperfine coupling constants in their EPR experiments. Excess electrons trapped on the oxide surface have also been studied as a promising way of tuning the electronic and magnetic properties.<sup>25</sup> Only a few theoretical studies of Li adsorption on MgO at higher coverage had been done to investigate the competition between the lateral interaction within Li adsorbates and the interface bonding between Li and MgO,<sup>51-53</sup> and little research had been done to study the growth mode of Li clusters and thin films on MgO, especially when considering the role of intrinsic defects on the MgO surface.

Recently, Zhu *et al.*<sup>26,31</sup> measured the differential adsorption heat for both Ca and Li deposition on a thick film of

MgO(100). They showed a striking difference between the growth of those two metals on the pristine and Ar<sup>+</sup> sputtered surfaces. The initial heat of adsorption for Ca [at 0.01 monolayer (ML)] is insensitive to sputtering while the initial heat for Li increases significantly on the sputtered surface. Our DFT calculations of Ca and Li on a variety of possible surface sites on MgO(100), combined with experimental measurements, were used to establish a model of defect distribution on the surface to explain the microcalorimetry adsorption thermodynamics.

In this paper, we provide the computational details comparing the adsorption of Li on MgO(100) to that of Ca and give some insight into why the two metals interact differently on the surface. This information, together with studies of transition metals, can provide a better understanding of the role of various defects during the particle and thin-film growth on MgO(100).

## II. CALCULATION METHODOLOGY

Our DFT calculations were carried out with a periodic supercell model using the Vienna *ab initio* simulation package, with the PW91 functional,<sup>54</sup> and projector-augmented-wave-based pseudopotentials.<sup>55</sup> A plane-wave cutoff of 250 eV, suitable for the pseudopotentials, was used. Spin polarization was checked and applied whenever necessary. Other details about the DFT calculations and the MgO(100) substrate models are the same as those in our work of Ca on MgO(100).<sup>30</sup>

A Bader *atoms-in-molecules* charge analysis<sup>56</sup> was conducted using a grid-based algorithm with core charges included in the calculations.<sup>57</sup> We define the charge on an atom as the difference between the Bader charge and its formal charge. We use the term charge transfer to mean a shift in the Bader charges, which does not necessarily correspond to the loss or gain of a whole electron; it can correspond to a local polarization between atoms. The charge on a vacancy is defined as the charge density in the Bader volume located in the vacancy. Diffusion barriers are calculated with the nudged elastic band<sup>58,59</sup> and dimer<sup>60</sup> methods.

Adsorption energies,  $E_{\text{ads}}$ , for a cluster of  $n$  Li atoms on the MgO surface are calculated as

$$-E_{\text{ads}} = E_{\text{sys}} - nE_{\text{Li}} - E_{\text{MgO}}, \quad (1)$$

where  $E_{\text{sys}}$  is the energy of  $n$  Li atoms adsorbed on the MgO surface,  $E_{\text{Li}}$  is the energy of an isolated Li atom, and  $E_{\text{MgO}}$  is the energy of the MgO substrate. The adsorption energy per Li atom is calculated as  $E_{\text{ads}}/n$ .

We also define a cluster binding energy to quantify the reaction energy when two clusters merge on the surface,

$$E_{\text{b}} = E_{\text{ads}}(n+m) - E_{\text{ads}}(n) - E_{\text{ads}}(m), \quad (2)$$

where  $E_{\text{ads}}(x)$  is the heat of adsorption for a cluster with  $x$  Li atoms.

## III. Li ADSORPTION ON THE TERRACE

### A. Monomer

The Li monomer binds to the MgO(100) terrace, such as Ca, only to the oxygen site [Fig. 1(a)]. We calculate an ad-

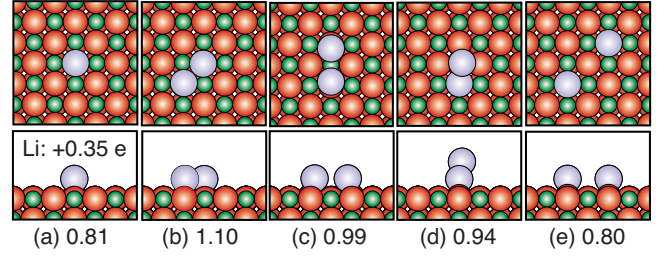


FIG. 1. (Color online) Li monomer and dimers on the MgO(100) surface, top and side views, (a) monomer; dimers: (b) D1; (c) D2; (d) D3; (e) D4. (Li atoms are large light blue circles; O are red and medium sized; Mg are green and small; adsorption energies are in electron volts per atom.)

sorption energy of 0.81 eV which compares well to previous DFT studies with different functionals (in parentheses): 0.83 eV (BLYP),<sup>52</sup> 1.07 eV (PBE96),<sup>52</sup> and 1.05 eV (B3LYP).<sup>28</sup> The electronic ground state is spin polarized. The Bader charge on Li is  $+0.35e$ ; upon adsorption, electron density flows from the Li atom to the surface atoms in the immediate vicinity of the adsorption site. Monomer diffusion occurs by hopping over the bridge site between two nearest-neighbor oxygen anions with a barrier of 0.47 eV. EPR experiments by Lian *et al.*<sup>27</sup> gave an estimate of the Li diffusion barrier to be 0.2 eV but that does not necessarily correspond to monomer diffusion—it could correspond to Li cluster diffusion as well.

### B. Dimer

The most stable Li dimer [D1 in Fig. 1(b)] binds to neighboring oxygen sites with a Li-Li distance of 2.81 Å ( $E_{\text{ads}} = 1.1$  eV/atom). In the gas phase, the Li dimer bond energy and length are calculated as 0.95 eV and 2.72 Å, respectively, as compared to experimental measurements at 1.13 eV and 3.03 Å.<sup>61</sup> Adsorption does not cause significant distortion to the gas phase dimer. Compared with two isolated monomers, the D1 dimer has a cluster binding energy of 0.58 eV, which is enough for the dimer to be stable on a time scale of milliseconds at room temperature. In contrast, the adsorbed Ca dimer bond length is significantly compressed

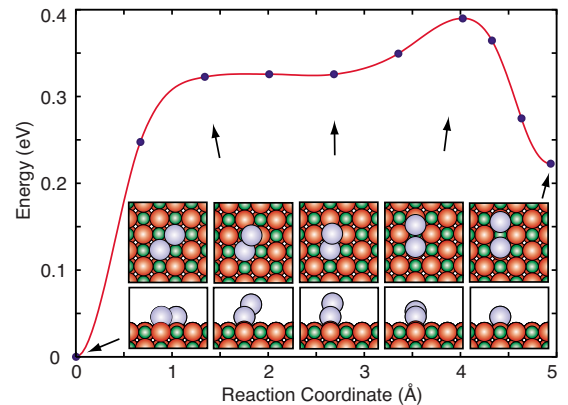


FIG. 2. (Color online) The most stable dimer D1 diffuses on the surface via two intermediate states (the vertical dimer D4 and the stretched dimer D2) with a barrier of 0.39 eV.

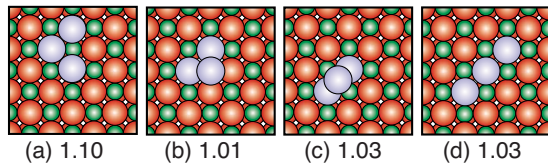


FIG. 3. (Color online) Li trimers: (a) flat triangle; (b) titled; (c) vertical; (d) linear.

from 4.13 Å in the gas phase, making the Ca dimer relatively less stable when adsorbed on the MgO surface.<sup>30</sup> The Li dimer diffuses through other stable intermediate states [see Figs. 1(c)–1(e)]. The lowest-energy diffusion pathway, shown in Fig. 2, has a barrier of 0.39 eV—lower than that of the monomer.

**C. Trimer**

There are four low-energy configurations of trimers on the surface. The flat triangle trimer is the most stable configuration with an adsorption heat of 1.10 eV/atom [Fig. 3(a)]. Compared to a monomer and dimer on the surface, the flat trimer has a cluster binding energy of 0.3 eV and a dissociation barrier of 0.77 eV. The flat trimer can diffuse by flipping with a barrier of only 0.26 eV to the vertical trimer, which in turn quickly flips back onto the surface with a barrier of 0.06 eV to a flat triangle at a new location (Fig. 4). Since the diffusion barrier is lower than dissociation, the trimer will diffuse as a cluster at room temperature. There is a shallow intermediate state [Fig. 3(b)] in the flipping diffusion pathway but it is less stable than the flat triangle. This trimer diffusion barrier is consistent with the activation energy of 0.2 eV estimated in EPR experiments.<sup>27</sup>

**D. Tetramer**

The flat square tetramer [Fig. 5(a)] is the most stable configuration ( $E_{ads}=1.13$  eV/atom) but there are other three-dimensional (3D) clusters which are nearly as stable [Figs. 5(b)–5(d)]. The flat tetramer has a cluster binding energy of 0.42 eV relative to a trimer and monomer on the surface, and a breakup barrier of 0.9 eV. It can convert into the tetrahedral structure with a barrier of 0.31 eV, indicating a fast transition between two-dimensional (2D) and 3D structures at room

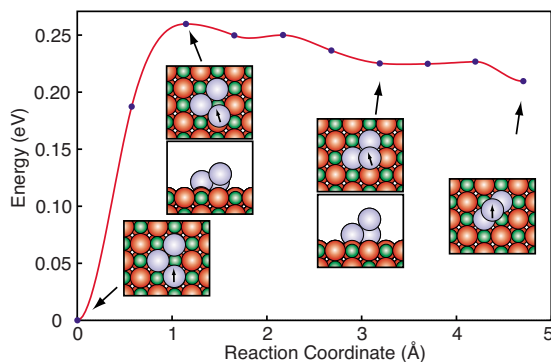


FIG. 4. (Color online) The flat triangle trimer diffuses by flipping to the vertical trimer with a barrier of 0.26 eV.

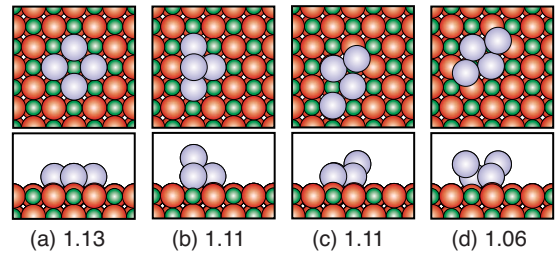


FIG. 5. (Color online) Li tetramers: (a) square; (b) tetrahedron; (c) crane; (d) boat.

temperature. The tetrahedron diffuses with a low barrier of 0.23 eV (Fig. 6). Therefore, the flat square can diffuse via the tetrahedron structure with the overall barrier of 0.31 eV, faster than monomer diffusion. The mobility of small clusters on MgO(100) has been seen for other metals including Ca, Pd, and Ag.<sup>30,62–66</sup>

**E. Pentamer**

The most stable pentamer [Fig. 7(b)] has a pyramidal shape with adsorption energy ( $E_{ads}=1.20$  eV/atom) and a cluster binding energy of 0.7 eV relative to a tetramer and monomer on the surface. Figure 7 shows how it can form from a “q”-shaped Li pentamer when a monomer meets a flat square on the surface with a barrier of 0.26 eV. The barrier for the Li adatom on the top of the pyramid to jump down to the surface is 0.40 eV so that the interconversion between the 2D and 3D structures is facile at room temperature.

**F. Larger clusters, islands, and monolayers**

We considered larger clusters (on a larger substrate) to investigate the relative stability between 2D and 3D islands (Fig. 8). The compact 3D clusters [Figs. 8(c) and 8(d)] are almost as stable as other less compact 3D or 2D clusters [Figs. 8(a) and 8(b)]. The Li monolayer epitaxially occupies each oxygen site on the MgO(100) surface. This is different from Ca, where the same number of atoms has to be accommodated in a bilayer due to the longer Ca-Ca bond length.<sup>30</sup> The adsorption energy of the Li monolayer is 1.5 eV/atom. Adding a Li adatom on top of the monolayer does not change

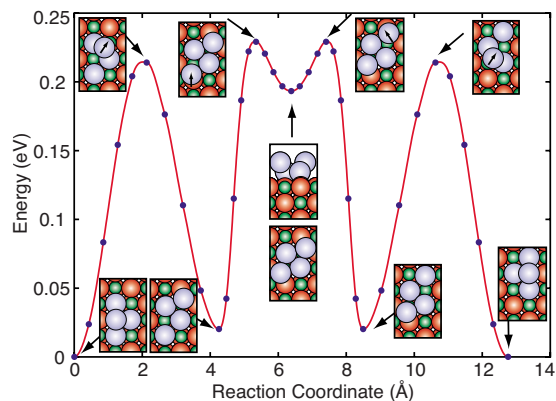


FIG. 6. (Color online) Diffusion of the Li tetramer with a barrier of 0.23 eV.

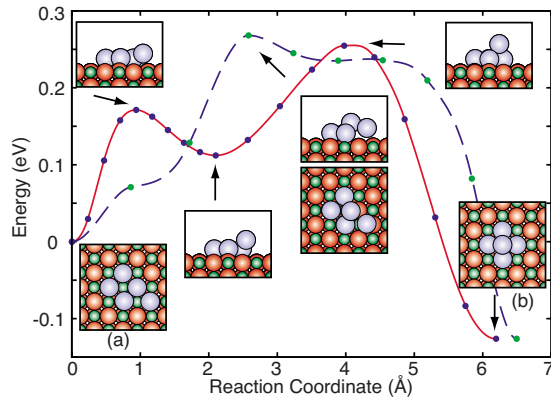


FIG. 7. (Color online) The transition of a flat q-shape pentamer into a pyramid by either a hop-up (dashed line) or push-up (solid line) mechanism.

the heat of adsorption per atom [Fig. 8(e)]. This indicates that Li can form either 2D or 3D islands on the terrace at high coverages, although 3D islands are slightly favored.

#### IV. POINT DEFECTS

##### A. F centers

There are two possible charge states of the oxygen vacancy (F center) on the MgO(100) surface.<sup>67,68</sup> The Li monomer binds weakly on the neutral F center with adsorption energy 0.57 eV [Fig. 9(a)], as compared to the terrace, 0.81 eV. A Bader analysis shows that there is  $+0.27e$  net charge on Li while the F center traps  $-1.2e$ . If the F center is positively charged [Fig. 9(b)], the Li monomer adsorbs strongly, with energy 1.37 eV, and the net charge on Li is  $+0.80e$ , with  $-1.1e$  trapped in the  $F^+$  center. Consistently, the Li atom is closer to the surface at the  $F^+$  than at the F center. The electronic ground state of Li on the F center is spin polarized but it is singlet on the  $F^+$  center due to pairing of the electron transferred from the Li to the surface and the electron in the vacancy. If a second Li monomer diffuses to a Li-filled  $F^+$  center, it will bind with 0.48 eV. Thus,  $F^+$  centers can nucleate Li clusters at room temperature.

In contrast, the adsorption of Ca to an  $F^+$  site is weaker than on terrace (0.76 and 0.84 eV, respectively) and a second Ca atom does not bind to the occupied  $F^+$  site so that Ca

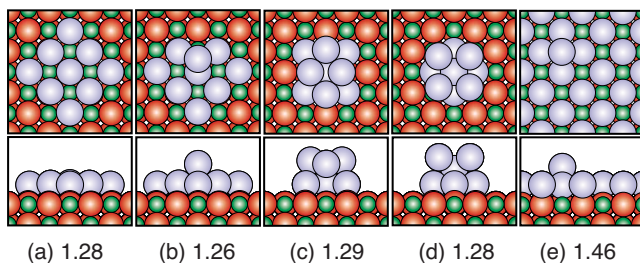


FIG. 8. (Color online) Nine-atom clusters [(a) 2D on nine oxygen sites, (b) 3D on eight oxygen sites, (c) 3D on five oxygen sites, and (d) 3D on four oxygen sites] at coverages of 9/32 and a monolayer island [(e) monolayer supporting a monomer].

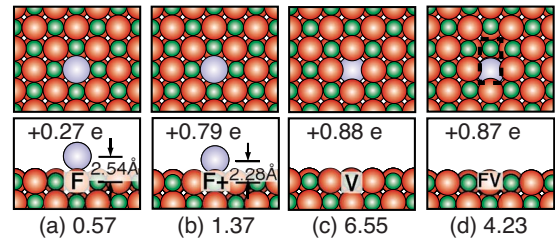


FIG. 9. (Color online) A Li monomer at (a) an F center; (b) an  $F^+$  center; (c) a V center; and (d) a divacancy (VF) center.

clusters will not nucleate.<sup>30</sup> A Bader charge analysis shows that the net charge is  $+0.23e$  for Ca/ $F^+$ , significantly less than  $+0.80e$  for Li. Figure 10 shows the charge-density difference caused by the adsorption of Li and Ca and the  $F^+$  center. More charge density is transferred from Li to the  $F^+$  center so that an electron pair is formed in the vacancy. In contrast, a smaller amount of charge is transferred from the Ca to a diffuse region instead being localized in the vacancy. The binding strength is correlated with the Bader charge transfer.

##### B. V centers

Another type of point defect is a Mg vacancy (V center). As shown in Fig. 9(c), the Li monomer goes into the V center. The net charge on the Li monomer is  $+0.88e$  and the heat of adsorption is large, 6.55 eV. Similarly, the Li monomer goes inside the Mg vacancy in a divacancy site (VF) and adsorbs strongly, 4.23 eV, with a similar net charge on Li  $+0.87e$  [Fig. 9(d)]. Unlike F centers, a Bader analysis shows that both the V and VF centers trap little electron density. This is at odds with previous DFT studies with an embedded cluster model,<sup>69</sup> which could be due to a tendency of pure DFT to delocalize charge. Additional Li adatoms adsorb strongly around the monomer-saturated V-type centers, which is not the case for Ca.<sup>30</sup>

#### V. STEPS

Other than point defects, there are also extended defects such as steps on the pristine MgO(100) surface.<sup>19</sup> The Li monomer adsorbs to an oxygen site at a step edge [Figs. 11(a) and 11(b)] with  $E_{\text{ads}}$  of 1.67 eV. This is close to the

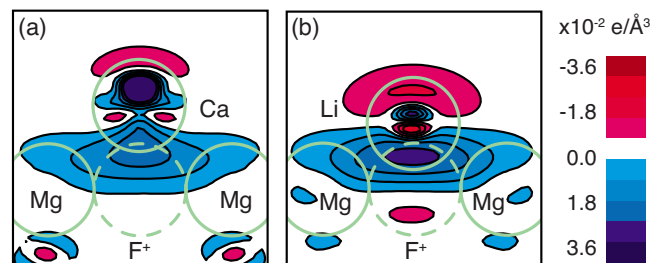


FIG. 10. (Color online) Charge-density difference of (a) Ca and (b) Li upon adsorption to a  $F^+$  center. Positive regions are electron density gain and negative are loss. Mg, Ca, and Li atoms are marked with solid circles;  $F^+$  centers are dashed.

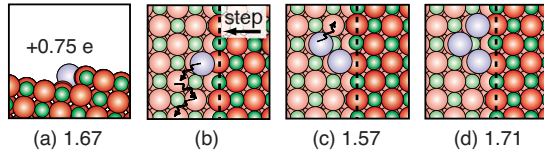


FIG. 11. (Color online) Li clusters at a step edge: (a) monomer side view; (b) monomer top view; (c) dimer and its diffusion path to a more stable structure ( $E_{\text{ads}}=1.87$  eV/atom); and (d) trimer.

binding energy at the reverse edge site, 1.65 eV, calculated with a cluster model using the B3LYP functional.<sup>28</sup> The net charge on Li is  $+0.75e$ . Similar to Ca diffusion along the step,<sup>30</sup> the Li monomer has to leave the step to an oxygen site on the terrace (barrier of 1.26 eV), before it diffuses back to the step edge (barrier of 0.40 eV) [see Fig. 11(b)]. A second Li monomer adsorbs strongly to a monomer bound to the step. This second monomer will cross a barrier of 0.20 eV to reach the neighboring empty step site and become the most stable dimer on the step edge via the wiggly path shown in Fig. 11(c). This process is irreversible at room temperature since the reverse process has a barrier of 0.81 eV. The trimer at the step edge [Fig. 11(d)] is also stable, with a cluster binding energy of 0.60 eV from the dimer against the step edge and a monomer on the terrace. These calculations indicate that at room temperature, Li will nucleate on empty step edges or clusters already formed there. This picture of nucleation agrees with speculations based on EPR experiments at 35 K.<sup>27,28</sup>

### A. Point defects in the step

The simplest defects in step edges are oxygen or magnesium vacancies.<sup>19</sup> Figure 12(a) shows how the Li monomer adsorbs against an oxygen vacancy in the step with a heat of adsorption of 1.6 eV that is only slightly less than on the perfect step. On the other hand, the Li monomer fills the Mg vacancy [Fig. 12(b)]. It appears that point defects on step edges are very similar to those on the terrace with respect to binding Li adatoms.

### B. Peroxo oxygen in the step

For MgO surfaces formed by oxidizing Mg at high temperature, peroxo groups are stable on step edges. The presence of these defects on metal oxides is supported by both experiments<sup>70,71</sup> and DFT calculations.<sup>72</sup> The O-O bond is

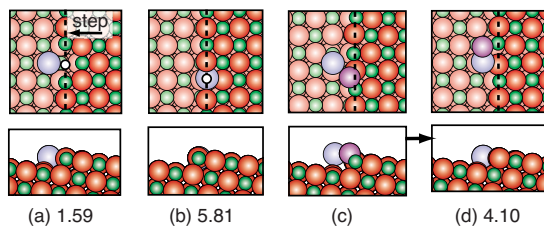


FIG. 12. (Color online) The Li monomer adsorbs at a point defect (white spot) at a step: (a) an F center; (b) a V center; (c) and (d) a peroxo atom (pink) incorporated in the step will spontaneously bind to a Li atom to form a Li-O pair at the step edge.

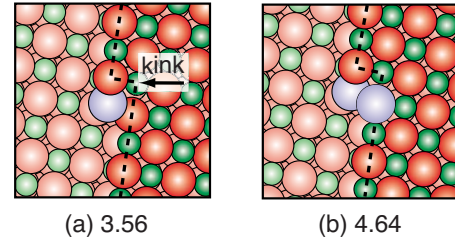


FIG. 13. (Color online) (a) A Li monomer adsorbs at an O kink site and (b) a second Li adatom adsorbs on top of the first.

stable as peroxo species at step edges<sup>30</sup> but the adsorption of a Li monomer near this oxygen-decorated step spontaneously breaks the peroxo oxygen bond to form a Li-O dimer [Figs. 12(c) and 12(d)], with an adsorption heat of 4.10 eV. This oxidation pattern of Li is the same as calculated for Ca.<sup>30</sup>

### C. Kinks

Imperfections of steps can create kink sites. A kink site is spanned by either three O or three Mg atoms. The Li adatom does not adsorb at a Mg kink but it binds strongly to an O kink site with energy 3.56 eV [Fig. 13(a)], both in agreement with the adsorption on reverse corner sites calculated by Finazzi *et al.*<sup>28</sup> The net charge on Li is  $+0.87e$ . As shown in Fig. 13(b), a second Li adatom can be captured by the monomer-filled kink site.

## VI. DISCUSSION

### A. Adsorption and growth of Li on the terrace

Li adatoms and small clusters bind strongly to the surface ( $E_{\text{ads}} > 0.8$  eV/atom) and have a high mobility, with diffusion barriers less than 0.5 eV. Only at very low temperature<sup>27,28</sup> will Li nucleate on the terrace. At room temperature, Li atoms deposited at rates of monolayer per second are able to diffuse to defects where clusters form. The high mobility is consistent with heat of adsorption measurements which are insensitive to the deposition flux.<sup>31,32</sup>

With increasing coverage, Li islands spread to terrace sites. In experiments by Farmer *et al.*,<sup>31</sup> the differential heat of adsorption reaches the bulk cohesion energy at coverages of 0.5 ML for Li and 0.3 ML for Ca, showing that the growth mode for both metals is not layer by layer. Instead, clusters form three-dimensional structures at submonolayer coverages as monomers add to existing islands. Our calculations show that the energy of 3D Li clusters is only somewhat more stable than 2D structures whereas Ca clusters strongly favor 3D clusters. It is expected, then, that Li reaches its bulk cohesion energy at higher coverage than Ca.

### B. Role of defects on Li adsorption and growth

Our calculations show that Li loses electronic density upon binding to the MgO(100) surface and that the magnitude of the Bader charge transfer correlates with the binding strength. This is the same trend that is found for Ca.<sup>30</sup> Therefore, any surface sites with electron deficiency should bind Li strongly. This has been demonstrated by strong binding at

vacancies involving Mg (V and VF centers) and sites with low coordination (steps, kinks, and peroxy species in steps). A good example of this trend is the comparison of Li adsorption on F and F<sup>+</sup> centers; the charged vacancy binds Li more than twice as strongly as the neutral vacancy. At room temperature, additional Li atoms bind to Li adatoms trapped at strong-binding defects. Small Li clusters can also serve as nucleation centers. This is qualitatively different from Ca since the Ca dimer is not stable and Ca adatoms will therefore seek out unoccupied strong-binding defect sites before forming larger clusters or islands.

A model of the defect distribution on MgO(100) was proposed to explain the measured differential adsorption heat for both Li and Ca growth.<sup>31</sup> The surface is divided into terraces by extended defects (presumably by steps) so that the strong-binding defects are localized to an area of the terrace. The size distribution of the terrace can be correlated with the different growth modes for Ca and Li to qualitatively reproduce the measured heat of adsorption during the thin-film growth.

### C. Growth mode for Li on MgO(100)

From both experimental and theoretical studies, we have the following picture for Li growth on MgO(100). At room temperature, Li atoms land on terrace regions confined by the surrounding extended defects (e.g., steps). Li atoms diffuse until a strong-binding site is reached, such as extended defects, F<sup>+</sup> centers if they are present, or to existing Li clusters. In this way, the heat of adsorption will drop from the initial value (with contributions from defects) to that of the Li bulk heat of sublimation.

The growth of Ca is qualitatively different from Li because Ca does not bind to defect sites with existing Ca atoms. Thus, the initial Ca heat of adsorption will be entirely due to binding at defects. These defects fill more rapidly with deposition, and the heat of adsorption drops more quickly to

the bulk heat of sublimation as 3D Ca clusters form.

This model was validated experimentally by creating a higher density of defects on the MgO surface with Ar<sup>+</sup> sputtering. With smaller terrace regions, the initial Li heat of adsorption increased because of Li binding at new defects whereas the initial heat of Ca adsorption did not change since it is already determined by the defects on the nonsputtered surface. Fitting this model to the experimental heats of adsorption for the two metals results in a semiquantitative distribution of defects on the MgO surface.<sup>31</sup>

## VII. CONCLUSIONS

We studied the adsorption of Li on the MgO(100) surface with DFT calculations. We found that Li adatoms bind weakly on the terrace and that small Li clusters are highly mobile at room temperature. The adsorption energy of Li on F<sup>+</sup> centers, V centers, steps, kinks, and even oxygen decorated edges is much stronger. At room temperature, Li clusters will nucleate at these strong-binding defects and grow islands that expand onto the terrace. In contrast with Ca, Li binds to F<sup>+</sup> centers and to existing islands at low coverage. The difference in these calculated energetics are important for understanding the differential adsorption heat curves measured in thin-film growth microcalorimetry experiments. This study provides an example of how the deposition of different metals can be used as probes that are sensitive to different surface defects.

## ACKNOWLEDGMENTS

This work was supported by the Robert A. Welch Foundation under Grant No. F-1601 and the National Science Foundation, Award No. CHE-0645497. The authors thank Charles T. Campbell for the helpful discussions. This work used computing resources at the Texas Advanced Computing Center.

\*henkelman@mail.utexas.edu

<sup>1</sup>T. Ito and J. H. Lunsford, *Nature (London)* **314**, 721 (1985).  
<sup>2</sup>J. H. Lunsford, *Angew. Chem., Int. Ed. Engl.* **34**, 970 (1995).  
<sup>3</sup>A. Zecchina, D. Scarano, S. Bordiga, G. Spoto, and C. Lamberti, *Adv. Catal.* **46**, 265 (2001).  
<sup>4</sup>A. Corma and S. Iborra, *Adv. Catal.* **49**, 239 (2006).  
<sup>5</sup>G. W. Huber, S. Iborra, and A. Corma, *Chem. Rev.* **106**, 4044 (2006).  
<sup>6</sup>C. T. Campbell, *Surf. Sci. Rep.* **27**, 1 (1997).  
<sup>7</sup>C. R. Henry, *Surf. Sci. Rep.* **31**, 231 (1998).  
<sup>8</sup>M. Bäumer and H.-J. Freund, *Prog. Surf. Sci.* **61**, 127 (1999).  
<sup>9</sup>G. Haas, A. Menck, H. Brune, J. V. Barth, J. A. Venables, and K. Kern, *Phys. Rev. B* **61**, 11105 (2000).  
<sup>10</sup>A. Bogicevic and D. R. Jennison, *Surf. Sci. Lett.* **515**, L481 (2002).  
<sup>11</sup>C. T. Campbell and D. E. Starr, *J. Am. Chem. Soc.* **124**, 9212 (2002).  
<sup>12</sup>L. Giordano, C. Di Valentin, J. Goniakowski, and G. Pacchioni,

*Phys. Rev. Lett.* **92**, 096105 (2004).

<sup>13</sup>J. A. Venables, L. Giordano, and J. H. Harding, *J. Phys.: Condens. Matter* **18**, S411 (2006).  
<sup>14</sup>L. Xu, C. T. Campbell, H. Jónsson, and G. Henkelman, *Surf. Sci.* **601**, 3133 (2007).  
<sup>15</sup>G. Renaud, R. Lazzari, C. Revenant, A. Barbier, M. Noblet, O. Ulrich, F. Leroy, J. Jupille, Y. Borensztein, C. R. Henry, J. P. Deville, F. Scheurer, J. Mane-Mane, and O. Fruchart, *Science* **300**, 1416 (2003).  
<sup>16</sup>G. Renaud, A. Barbier, and O. Robach, *Phys. Rev. B* **60**, 5872 (1999).  
<sup>17</sup>P. V. Sushko, A. L. Shluger, and C. R. A. Catlow, *Surf. Sci.* **450**, 153 (2000).  
<sup>18</sup>C. Barth and C. R. Henry, *Phys. Rev. Lett.* **91**, 196102 (2003).  
<sup>19</sup>M. Sterrer, E. Fischbach, T. Risse, and H.-J. Freund, *Phys. Rev. Lett.* **94**, 186101 (2005).  
<sup>20</sup>S. Benedetti, H. M. Benia, N. Nilius, S. Valeri, and H.-J. Freund, *Chem. Phys. Lett.* **430**, 330 (2006).

- <sup>21</sup>H. M. Benia, P. Myrach, and N. Nilius, *New J. Phys.* **10**, 013010 (2008).
- <sup>22</sup>S. Benedetti, P. Torelli, S. Valeri, H. M. Benia, N. Nilius, and G. Renaud, *Phys. Rev. B* **78**, 195411 (2008).
- <sup>23</sup>S. Brazzelli, C. Di Valentin, G. Pacchioni, E. Giamello, and M. Chiesa, *J. Phys. Chem. B* **107**, 8498 (2003).
- <sup>24</sup>M. Chiesa, E. Giamello, C. Di Valentin, G. Pacchioni, Z. Sojka, and S. Van Doorslaer, *J. Am. Chem. Soc.* **127**, 16935 (2005).
- <sup>25</sup>M. Chiesa, M. C. Paganini, E. Giamello, D. M. Murphy, C. Di Valentin, and G. Pacchioni, *Acc. Chem. Res.* **39**, 861 (2006).
- <sup>26</sup>J. F. Zhu, J. Farmer, N. Ruzycski, L. Xu, C. T. Campbell, and G. Henkelman, *J. Am. Chem. Soc.* **130**, 2314 (2008).
- <sup>27</sup>J. C. Lian, E. Finazzi, C. Di Valentin, T. Risse, H. J. Gao, G. Pacchioni, and H.-J. Freund, *Chem. Phys. Lett.* **450**, 308 (2008).
- <sup>28</sup>E. Finazzi, C. Di Valentin, G. Pacchioni, M. Chiesa, E. Giamello, H. J. Gao, J. C. Lian, T. Risse, and H.-J. Freund, *Chem.-Eur. J.* **14**, 4404 (2008).
- <sup>29</sup>U. Martinez, L. Giordano, and G. Pacchioni, *J. Chem. Phys.* **128**, 164707 (2008).
- <sup>30</sup>L. Xu and G. Henkelman, *Phys. Rev. B* **77**, 205404 (2008).
- <sup>31</sup>J. A. Farmer, C. T. Campbell, L. Xu, and G. Henkelman, *J. Am. Chem. Soc.* **131**, 3098 (2009).
- <sup>32</sup>J. A. Farmer, N. Ruzycski, J. F. Zhu, and C. T. Campbell, *Phys. Rev. B* **80**, 035418 (2009).
- <sup>33</sup>P. Myrach, N. Nilius, and H.-J. Freund, *J. Phys. Chem. C* **113**, 18740 (2009).
- <sup>34</sup>J. H. Lunsford, *Catal. Today* **6**, 235 (1990).
- <sup>35</sup>M. C. Wu, C. M. Truong, K. Coulter, and D. W. Goodman, *J. Am. Chem. Soc.* **114**, 7565 (1992).
- <sup>36</sup>C. Trionfetti, I. V. Babich, K. Seshan, and L. Lefferts, *Langmuir* **24**, 8220 (2008).
- <sup>37</sup>V. K. Diez, C. R. Apesteguia, and J. I. di Cosimo, *J. Catal.* **240**, 235 (2006).
- <sup>38</sup>R. Orlando, F. Cora, R. Millini, G. Perego, and R. Dovesi, *J. Chem. Phys.* **105**, 8937 (1996).
- <sup>39</sup>L. Ackermann, J. D. Gale, and C. R. A. Catlow, *J. Phys. Chem. B* **101**, 10028 (1997).
- <sup>40</sup>H. Aritani, H. Yamada, T. Nishio, T. Shiono, S. Imamura, M. Kudo, S. Hasegawa, T. Tanaka, and S. Yoshida, *J. Phys. Chem. B* **104**, 10133 (2000).
- <sup>41</sup>L. K. Dash and M. J. Gillan, *Surf. Sci.* **549**, 217 (2004).
- <sup>42</sup>M. Nolan and G. W. Watson, *Surf. Sci.* **586**, 25 (2005).
- <sup>43</sup>N. Zobel and F. Behrendt, *J. Chem. Phys.* **125**, 074715 (2006).
- <sup>44</sup>M.-C. Wu, C. M. Truong, and D. W. Goodman, *Phys. Rev. B* **46**, 12688 (1992).
- <sup>45</sup>A. Lichanot, C. Larrieu, C. Zicovich-Wilson, C. Roetti, R. Orlando, and R. Dovesi, *J. Phys. Chem. Solids* **59**, 1119 (1998).
- <sup>46</sup>H. Matsuhashi, M. Oikawa, and K. Arata, *Langmuir* **16**, 8201 (2000).
- <sup>47</sup>M. M. Tardío, R. Ramírez, R. González, and Y. Chen, *Phys. Rev. B* **66**, 134202 (2002).
- <sup>48</sup>A. van Veen, M. A. van Huis, A. V. Fedorov, H. Schut, F. Labohm, B. J. Kooi, and J. T. M. de Hosson, *Nucl. Instrum. Methods Phys. Res. B* **191**, 610 (2002).
- <sup>49</sup>T. Berger, J. Schuh, M. Sterrer, O. Diwald, and E. Knozinger, *J. Catal.* **247**, 61 (2007).
- <sup>50</sup>D. O. Scanlon, A. Walsh, B. J. Morgan, and G. W. Watson, *e-J. Surf. Sci. Nanotechnol.* **7**, 395 (2009).
- <sup>51</sup>D. R. Alfonso, J. E. Jaffe, A. C. Hess, and M. Gutowski, *Surf. Sci.* **466**, 111 (2000).
- <sup>52</sup>J. A. Snyder, J. E. Jaffe, M. Gutowski, Z. Lin, and A. C. Hess, *J. Chem. Phys.* **112**, 3014 (2000).
- <sup>53</sup>V. G. Zavodinsky and A. Kiejna, *Surf. Sci.* **538**, 240 (2003).
- <sup>54</sup>J. P. Perdew, in *Electronic Structure of Solids*, edited by P. Ziesche and H. Eschrig (Akademie Verlag, Berlin, 1991), pp. 11–20.
- <sup>55</sup>G. Kresse and D. Joubert, *Phys. Rev. B* **59**, 1758 (1999).
- <sup>56</sup>R. F. W. Bader, *Atoms in Molecules: A Quantum Theory* (Oxford University Press, New York, 1990).
- <sup>57</sup>W. Tang, E. Sanville, and G. Henkelman, *J. Phys.: Condens. Matter* **21**, 084204 (2009).
- <sup>58</sup>G. Henkelman, B. P. Uberuaga, and H. Jónsson, *J. Chem. Phys.* **113**, 9901 (2000).
- <sup>59</sup>G. Henkelman and H. Jónsson, *J. Chem. Phys.* **113**, 9978 (2000).
- <sup>60</sup>G. Henkelman and H. Jónsson, *J. Chem. Phys.* **111**, 7010 (1999).
- <sup>61</sup>D. R. Lide, *CRC Handbook of Chemistry and Physics*, 87th ed. (CRC Press, New York, 2006).
- <sup>62</sup>L. Xu, G. Henkelman, C. T. Campbell, and H. Jónsson, *Phys. Rev. Lett.* **95**, 146103 (2005).
- <sup>63</sup>L. Xu, G. Henkelman, C. T. Campbell, and H. Jónsson, *Surf. Sci.* **600**, 1351 (2006).
- <sup>64</sup>G. Barcaro, A. Fortunelli, F. Nita, and R. Ferrando, *Phys. Rev. Lett.* **95**, 246103 (2005).
- <sup>65</sup>G. Barcaro and A. Fortunelli, *New J. Phys.* **9**, 22 (2007).
- <sup>66</sup>R. Ferrando and A. Fortunelli, *J. Phys.: Condens. Matter* **21**, 264001 (2009).
- <sup>67</sup>G. Pacchioni, *ChemPhysChem* **4**, 1041 (2003).
- <sup>68</sup>J. Carrasco, N. Lopez, F. Illas, and H.-J. Freund, *J. Chem. Phys.* **125**, 074711 (2006).
- <sup>69</sup>D. Ricci, G. Pacchioni, P. V. Sushko, and A. L. Shluger, *J. Chem. Phys.* **117**, 2844 (2002).
- <sup>70</sup>C. Hess and J. H. Lunsford, *J. Phys. Chem. B* **106**, 6358 (2002).
- <sup>71</sup>M. Nakamura, H. Mitsuhashi, and N. Takezawa, *J. Catal.* **138**, 686 (1992).
- <sup>72</sup>C. Di Valentin, R. Ferullo, R. Binda, and G. Pacchioni, *Surf. Sci.* **600**, 1147 (2006).